

Dyons and Roberge - Weiss transition in lattice QCD

Vitaly Bornyakov

IHEP, Protvino and ITEP, Moscow and FEFU, Vladivostok

Quark Confinement and the Hadron Spectrum XII
Thessaloniki 30.08.16

Outline:

- Introduction
- Roberge-Weiss transition
- Calorons and dyons
- Spectral gap
- Conclusions

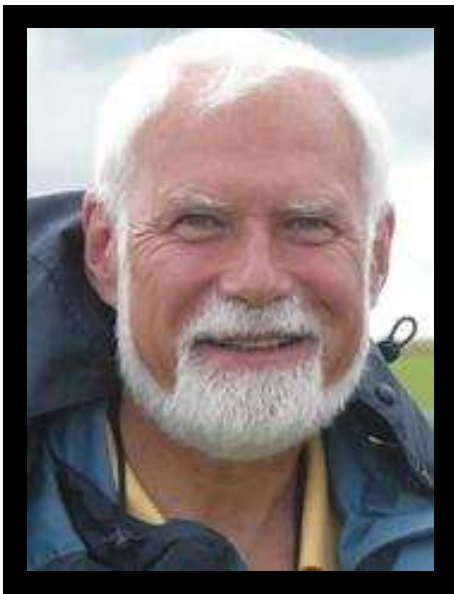
In collaboration with

FEFU lattice group:

Atsushi Nakamura, Alexander Molochkov, Vladimir Goy,
Alexander Nikolaev, Denis Boyda

and

Michael Ilgenfritz [JINR, Dubna](#)
Boris Martemyanov [ITEP, Moscow](#)



FEFU lattice QCD group

Web site <http://188.162.234.56/>

- Main project: Study of the quark-gluon plasma using lattice QCD
- Supported by Russian Science Foundation grant
- Leader: prof. A. Nakamura
- Main goals: phase diagram of QCD in (μ_B, T) plain

Two more talks at this conference:

Alexander Molochkov, *Thursday, Section A, Focus Subsection*

Alexander Nikolaev, *Friday, Deconfinement*

Our machine :

10 nodes (2 Intel E5-2680-v2, 64Gb; 2 x NVidia Tesla K40X Kepler)
23.52TFlops (Linpack)

HMC code for GPU from scratch

Its performance is comparable to QUDA code

We simulate $N_f = 2$ lattice QCD with improved Wilson fermions and Iwasaki improved gauge field action

$T = 0$ input is taken from WHOT QCD collaboration results
Currently quark mass is defined by relation $m_\pi/m_\rho = 0.8$
Lattice size: $16^3 \times 4$

Main goal: to obtain the phase diagram of QCD at finite baryon density

Our approach to finite density QCD: canonical ensemble approach
We simulate at imaginary chemical potential $\mu_q = i\mu_q^I$

At $T > T_c$ ($T = 1.35 T_c$)

at $T < T_c$ ($T = 0.93 T_c$)

Results, presented in this talk is a byproduct of the project on finite density QCD

Results to be presented by Alexander Nikolaev on Friday

Roberge-Weiss transition

Roberge, Weiss, 1986

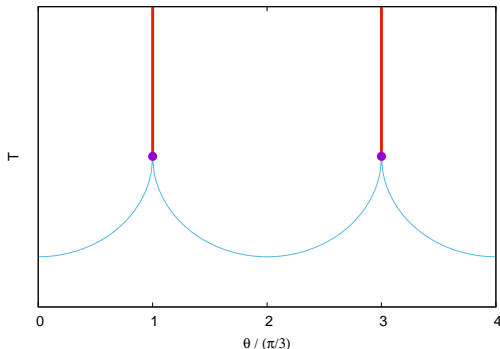
Why imaginary quark chemical potential ?

At imaginary chemical potential $\mu_q = i|\mu_{qI}|$ the sign problem is absent and standard Monte Carlo algorithms can be applied to simulate lattice QCD

QCD possesses rich phase structure at nonzero $\theta \equiv \mu_{qI}/T$, which depends on the number of flavors N_f and the quark mass m_q

Study of QCD at nonzero θ can provide us with information about physical range: $\mu_q = 0$ and even about $\mu_q > 0$

- Canonical ensemble approach
- extrapolation to $\mu_q = 0$ or analytical continuation to nonzero real μ_q

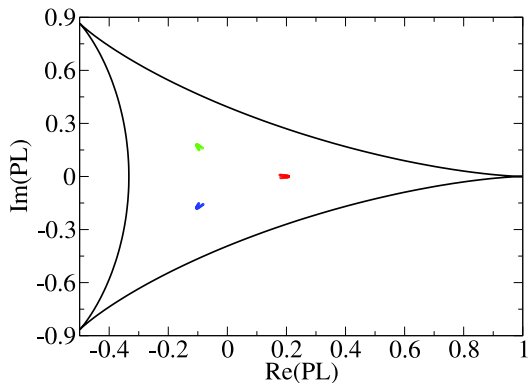


The QCD partition function Z is a periodic function of $\theta = \mu_{qI}/T$:

$$Z(\theta) = Z(\theta + 2\pi/N_c) \quad (1)$$

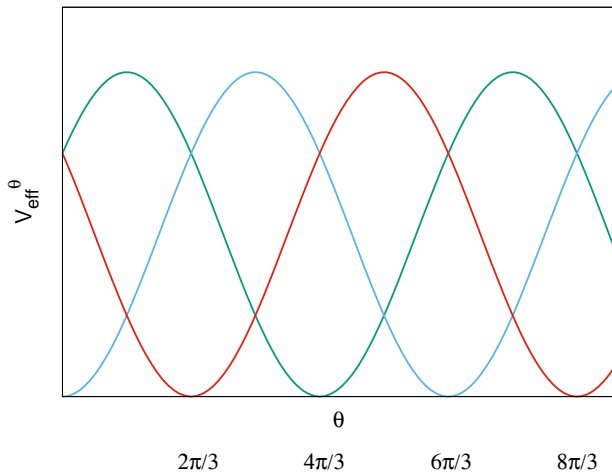
There are 1st order phase transitions at $\theta = (2k + 1)\pi/3$ at $T > T_{RW} > T_c$

These are transitions between $Z(3)$ sectors of the theory. A particular sector can be identified by the phase of the Polyakov loop.



Polyakov loop scatter plot at $T/T_c = 1.35$ and $-\pi < \theta < \pi$.

RW result for the perturbative effective potential:



Important note

The θ dependence of the fermionic determinant can be eliminated from the Dirac operator and transferred to the boundary conditions

$$\psi(\mathbf{x}, t) \rightarrow e^{it\theta T} \psi(\mathbf{x}, t) \quad (2)$$

The determinant is invariant under simultaneous nonperiodic gauge transformation $g(\mathbf{x}, t)$:

$$g(\mathbf{x}, 1/T) = e^{i2\pi/3} g(\mathbf{x}, 0) \quad (3)$$

and shift in θ by $2\pi/3$ (or respective shift in bc).

Calorons and Dyons

Instantons at $T = 0$ are known since 1975 - BPST instantons

Belavin, Polyakov, Schwartz, and Tyupkin

Models of QCD vacuum based on this solution - instanton gas and instanton liquid models - were developed (Shuryak; Diakonov)

At $T > 0$ analogous instanton solution - Harrington-Shepard caloron with trivial holonomy

semiclassical treatment of the Yang-Mills partition function has been formulated by Gross, Pisarski and Yaffe based on this caloron solution

$$A_{\mu}^a \text{ (HS)}(\mathbf{x}) = \eta_{a\mu\nu}^{(\pm)} \partial_{\nu} \log \Phi(\mathbf{x}) \quad (4)$$

The untraced Polyakov loop at spatial infinity becomes an element of the center $\mathbf{Z}(N)$ of $SU(N)$,

$$\mathbf{P} \exp \left(i \int_0^b A_4(\vec{x}, x_4) dx_4 \right) \Big|_{|\vec{x}| \rightarrow \infty} \Longrightarrow \mathcal{P}_{\infty} \in \mathbf{Z}(N) \quad (5)$$

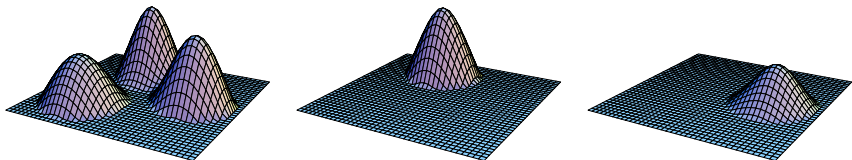
About 20 years ago another finite temperature solution was discovered:

KvBLL caloron Kraan and van Baal, 1998; Lee and Lu, 1998

periodic instantons (calorons) with nontrivial holonomy

$$\mathcal{P}_\infty \notin \mathbf{Z}(N) \quad (6)$$

Such a caloron has $Q_t = 1$ but consists of N_c fractionally charged monopole constituents which turn into static (with respect to x_4) BPS monopoles, if the constituents are sufficiently separated from each other

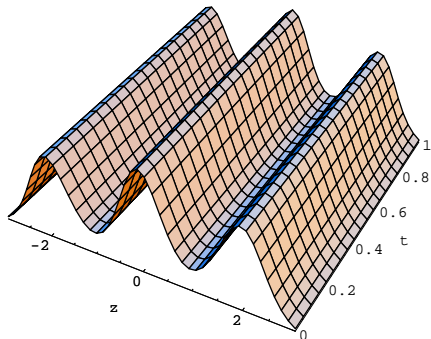


Left: Slice of the action density at fixed x_4 for a single $SU(3)$ KvBLL caloron with non-trivial holonomy: three static monopole constituents well separated from each other.

Center: Localisation of the zero mode for antiperiodic boundary conditions

Right: Same as in Center but for periodic boundary conditions

The figures are from Pierre van Baal's talk, Dubna, 1999

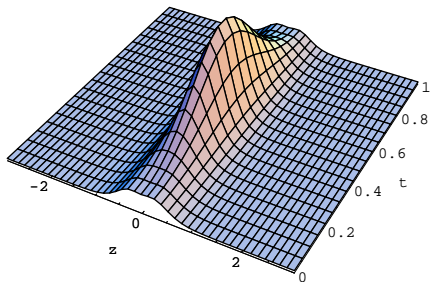


Because of their (anti)selfduality these monopoles are usually called dyons.

Their action is fully determined by the eigenvalues of the asymptotic holonomy \mathcal{P}_∞ and constitute together the one-instanton action

$S_{\text{inst}} = 8\pi^2/g^2$ of the caloron.

In the opposite limit, where the constituents are located near to each other, the action and the topological charge density of the KvBLL solution looks very similar to that of a HS caloron (or BPST instanton), i.e. concentrated within one lump of action and topological charge.



For $SU(3)$ calorons holonomy is parameterized:

$$\mathcal{P}_\infty = \text{diag}(e^{2\pi i\mu_1}, e^{2\pi i\mu_2}, e^{2\pi i\mu_3}), \quad (7)$$

with $\mu_1 \leq \mu_2 \leq \mu_3 \leq \mu_4 = 1 + \mu_1$,
 $\mu_1 + \mu_2 + \mu_3 = 0$.

Let \vec{y}_1 , \vec{y}_2 and \vec{y}_3 be three 3D position vectors of dyons remote from each other.

Then a caloron consists of three lumps carrying the instanton action split into fractions

$m_1 = \mu_2 - \mu_1$, $m_2 = \mu_3 - \mu_2$, $m_3 = \mu_4 - \mu_3$,
 concentrated near the \vec{y}_j .

Two important properties :

- at positions of dyon constituents at least two eigenvalues of the **local** holonomy are degenerate

Kraan, van Baal, 1998

- the zero mode of the massless Dirac operator in a KvBLL caloron background is localized only around one of the constituents

Chernodub, van Baal, 1999, Bruckmann, van Baal, 2003

On which dyon this happens depends on the boundary condition applied to the fermion field in the Euclidean time direction

For the case of maximally nontrivial holonomy (deeply in the confinement phase we have degenerate masses

$$m_1 = m_2 = m_3 = 1/3 \text{ and } \mu_1 = 1/3, \mu_2 = 0, \mu_3 = 1/3.$$

For $\phi \in [2\pi/3, 0]$, the zero mode is located on the first dyon and for $\phi = \pi/3$ its localization is maximal.

For $\phi = \pi/3$ and $\phi = \pi$ it is maximal on the second and third dyon, respectively.

On the contrary, for the limiting case of maximally trivial holonomy (deeply in the deconfinement phase) we obtain asymmetrical constituent masses $m_1 = m_2 = 0, m_3 = 1$.

The localization of the only massive constituent is then observed with the zero mode related to the antiperiodic boundary condition $\phi = \pi$.

Change of the single zero mode's localization with the change of boundary conditions was observed in lattice simulations below and above T_c

For $SU(2)$ and $SU(3)$ lattice gauge theory this property of mobility (with changing degree of localization) is shared also by a band of near-zero modes of the overlap Dirac operator

VB, Ilgenfritz, Matemyanov, Müller-Preussker, 2007, 2008, 2014
 Ilgenfritz, Matemyanov, Müller-Preussker, 2013

Thus, not only zero modes but the band of low lying modes of the overlap Dirac operator identified with different boundary conditions can be used as an effective tool to detect distinct topological objects.

Additional indicators of calorons/dyons:

- high values of the topological charge density
- Abelian monopoles found after fixing MAG

All these properties were used to detect calorons and/or dyons in MC generated thermal lattice gauge field configurations after some cooling or 4D APE smearing or overlap operator mode expansions for $SU(2)$ and $SU(3)$ pure gauge theory as well as for lattice QCD

Lattice studies of calorons and dyons led to the following picture of the topological structure of thermal Yang-Mills fields in terms of (anti)calorons and (anti)dyons:

For $T < T_c$, where the spatially averaged Polyakov loop in gluodynamics is fluctuating around zero, we see all possible dyon constituents with equal statistical weight, as one would expect them in a KvBLL caloron with maximally non-trivial (asymptotic) holonomy ($L = \frac{1}{3} \text{Tr } P = 0$).

For $T > T_c$, where the Polyakov loop average tends to $SU(N_c)$ center values and where one might expect caloron configurations with holonomies close to such values, topological clusters identifiable with corresponding heavy dyon constituents are statistically suppressed

As a consequence, on one hand (anti)calorons – containing necessarily heavy and light (anti)dyons in this case – are rare, what explains the decreasing topological susceptibility with rising temperature.

On the other hand, clusters, which can be interpreted (with the triggers mentioned above) as light dyons are abundant

$SU(2)$: VB, Ilgenfritz, Matemyanov, Muller-Preussker, 2008

$SU(3)$: Ilgenfritz, Martemyanov, Müller-Preussker, 2013

VB, Ilgenfritz, Matemyanov, Müller-Preussker, 2013, 2014

The dissociation of KvBLL calorons into dyon constituents has led to the hope to describe quark confinement at $T < T_c$ in terms of a liquid of correlated BPS monopoles or dyons

Work in this direction was done over recent years by few groups:

Gerhold, Ilgenfritz, Müller-Preussker, 2007

lattice simulation of confining gas of calorons (dyon pairs in $SU(2)$)

Diakonov, Petrov, 2007

confining gas of dyons with quantum interaction

Bruckmann, Dinter, Ilgenfritz, Maier, Müller-Preussker, Wagner, 2012

confining gas of noninteracting dyons

Shuryak and collaborators, 2012-2016

dyon chiral symmetry breaking, confinement and

confinement-deconfinement transition with interaction instanton-dyon

ensembles

(talks by E. Shuryak (plenary) and R. Larsen (this session))

The overlap Dirac operator D

Neuberger, 1998

$$\begin{aligned}
 D(m=0) &= \frac{\rho}{a} \left(1 + \frac{D_W}{\sqrt{D_W^\dagger D_W}} \right) \\
 &= \frac{\rho}{a} (1 + \text{sgn}(D_W)) , \tag{8}
 \end{aligned}$$

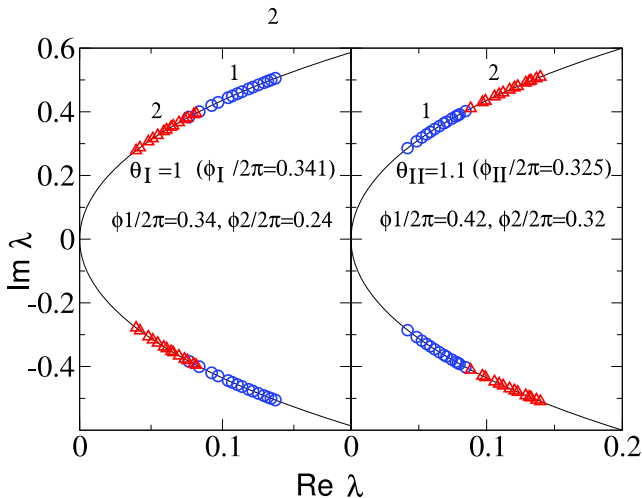
where

$$D_W = M - \rho/a,$$

M is the hopping term of the Wilson-Dirac operator

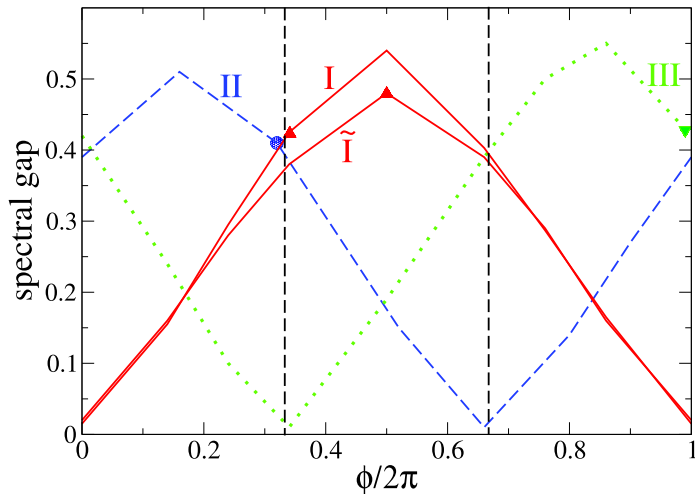
ρ/a is a negative mass term

The non-zero modes appear in pairs, which are related to each other by $\psi_\lambda = \gamma_5 \psi_{-\lambda}$, and have vanishing chirality.

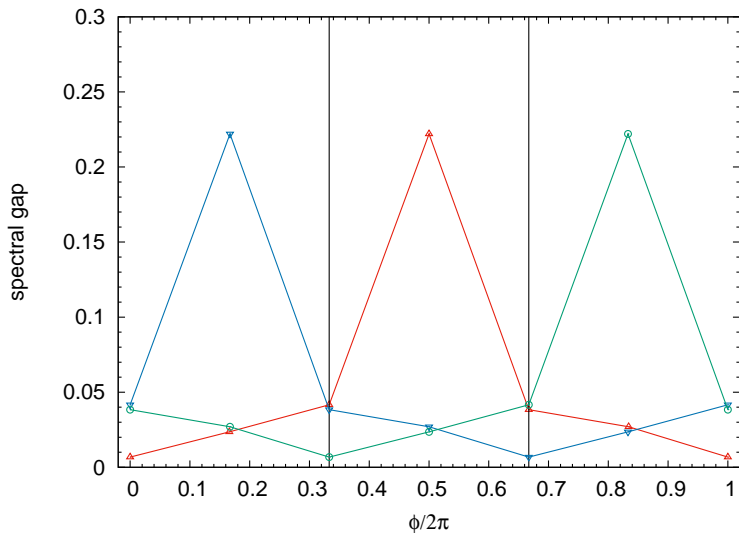


Spectrum of the overlap massless lattice Dirac operator for two MC configurations on both sides of RW transition.

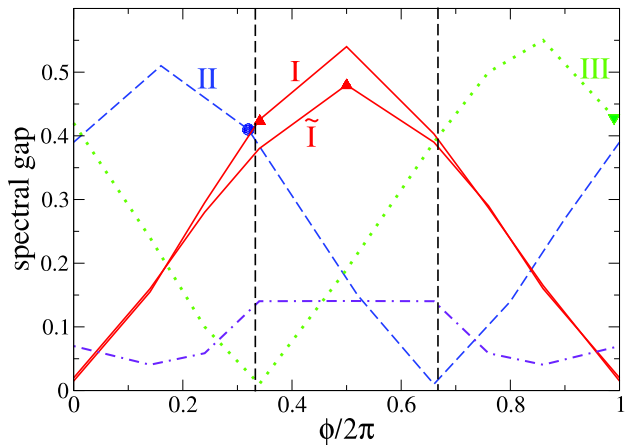
$T/T_c = 1.35, \theta_I = 1.0 < \pi/3, \theta_{II} = 1.1 > \pi/3.$



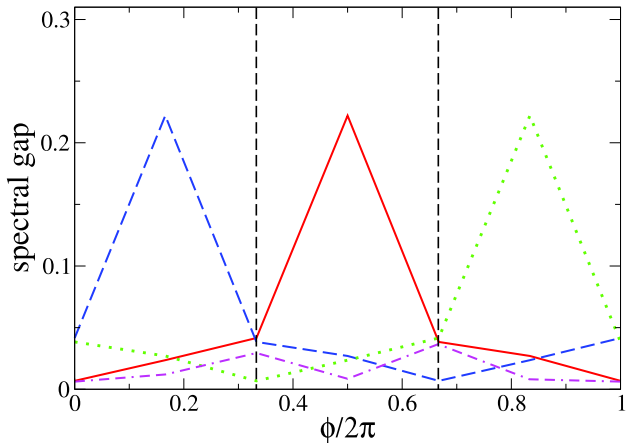
Spectral gap for MC configurations. $\phi \equiv \pi - \theta$



Spectral gap for double dyon-antidyon configuration.



Spectral gap comparison for confinement and deconfinement.



Spectral gap comparison for double dyon-antidyon configuration and caloron - anticaloron configuration.

Conclusions

We computed the overlap Dirac operator low modes spectrum in lattice QCD with $N_f = 2$ of improved Wilson fermions at $T/T_c = 1.35$, $m_\pi/m_\rho = 0.8$ at nonzero imaginary chemical potential.

We consider equilibrium configurations generated at particular values of imaginary chemical potential taken from all 3 center sectors. We compute 20 lowest modes of the Dirac operator for every such configuration varying imaginary chemical potential in the Dirac equation.

We observed that the spectral gap has some characteristic features for equilibrium configuration generated at chemical potential θ from given center sector. Namely this gap

- has a maximum in the middle of the sector and decreases monotonously;
- this behavior is independent of the particular value of θ inside the sector at which the MC configuration was generated;

- spectral gaps for two sectors intersect at the boundary between them.

This implies that configurations generated at θ from one sector have low statistical weight in another sector.

We compare with spectral gap computed for the double dyon-anti-dyon configuration and find similar behavior.

We consider this similarity as indication of the contribution of dyons into the RW transition.

We show that in the confinement phase the situation is qualitatively different.